Published in final edited form as:
Brain Res. 2014 November 24; 1590: 85–96. doi:10.1016/j.brainres.2014.09.067.

The effects of aging, housing and ibuprofen treatment on brain neurochemistry in a triple transgene Alzheimer's disease mouse model using magnetic resonance spectroscopy and imaging

Ji-Kyung Choi[1], **Isabel Carreras**[2,3], **Nur Aytan**[2], **Eric Jenkins-Sahlin**[1], **Alpaslan Dedeoglu**[1,2,3,*], and **Bruce G. Jenkins**[1,*]

[1]Martinos Center for Biomedical Imaging, Department of Radiology, Massachusetts General Hospital and Harvard Medical School, Boston, Massachusetts 02114

[2]Department of Veterans Affairs, VA Boston Healthcare System, Boston, Massachusetts 02130

[3]Department of Biochemistry, Boston University School of Medicine, Boston, Massachusetts 02118

[4]Department of Neurology, Boston University School of Medicine, Boston, Massachusetts 02118

Abstract

We investigated a triple transgene Alzheimer's disease (AD) mouse model that recapitulates many of the neurochemical, anatomic, pathologic and behavioral defects seen in human AD. We studied the mice as a function of age and brain region and investigated potential therapy with the non-steroidal anti-inflammatory drug ibuprofen. Magnetic resonance spectroscopy (MRS) showed alterations characteristic of AD (i.e. increased myo-inositol and decreased N-acetylaspartate (NAA)). Mice at 6 months of age showed an increase in myo-inositol in the hippocampus at a time when the Aβ is intracellular, but not in amygdala or cortex. Myo-inositol increased as a function of age in the amygdala, cortex and striatum while NAA decreased only in the hippocampus and cortex at 17–23 months of age. Ibuprofen protected the increase of myo-inositol at six months of age in the hippocampus, but had no effect at 17–23 months of age (a time when Aβ is extracellular). *In vivo* MRI and MRS showed that at 17–23 months of age there was a significant protective effect of ibuprofen on hippocampal volume and NAA loss. Together, these data show the following: the increase in myo-inositol occurs before the decrease in NAA in hippocampus but not cortex; the hippocampus shows earlier changes than does the amygdale or cortex consistent with earlier deposition of Aβ40–42 in the hippocampus and ibuprofen protects against multiple components of the AD pathology. These data also show a profound effect of housing on this particular mouse model.

Address Correspondence to: Ji-Kyung Choi or Bruce G. Jenkins, PhD, A. A. Martinos Center for Biomedical Imaging, Dept. Radiology, Massachusetts General Hospital and Harvard Medical School, Building 149, 13th Street, Charlestown MA, 02129. jchoi@nmr.mgh.harvard.edu or bgj@nmr.mgh.harvard.edu. Telephone: 617-726-5816, Fax: 617-726-7422.
*Contributed equally to the study

Introduction

The cost of Alzheimer's disease (AD), both in human and financial terms, is expected to place an increasing, essentially unsustainable, burden on healthcare systems worldwide due to aging populations. It is crucial to find potential therapies that can either prevent the disease or slow progression. Epidemiologic studies of patients treated with non-steroidal anti-inflammatory drugs (NSAIDs) for at least 24 months showed a large decreased subsequent relative risk of AD (in t' Veld et al., 2001; Stewart et al., 1997). Studies in Alzheimer's disease mouse models have shown protection against various aspects of behavioral and pathologic markers using NSAIDs (McGeer and McGeer, 2007) although clinical studies with patients who already have AD have been less successful (Jaturapatporn et al., 2012; Mullane and Williams, 2013). We showed using both magnetic resonance spectroscopy (MRS), as well as post-mortem histopathology that we could protect neuronal elements of the pathology in aged mice using treatment with ibuprofen in a double transgenic mouse model (PS1×APP), although not all markers were responsive to the treatment (Choi et al., 2010b). This neuronal protection correlated with decreased Aβ plaque deposition. We also showed that treatment of triple transgene mice with ibuprofen was able to decrease not only the Aβ pathology but also hyper-phosphorylated tau (McKee et al., 2008). Magnetic resonance imaging and spectroscopy can provide non-invasive windows onto the neurodegenerative process and have become invaluable in assessing the impact of potential therapies in AD (Choi et al., 2007; Jack, 2012; Johnson et al., 2012; Westman et al., 2010).

MRS can provide information on both neuronal health and viability using the marker N-acetylaspartate (NAA) and also can provide information on glial markers such as myo-inositol a chemical that is elevated in both AD mouse models (Dedeoglu *et al.*, 2004;(Choi et al., 2010b; Marjanska et al., 2005; Mlynarik et al., 2012; von Kienlin et al., 2005) as well as in humans (Kantarci et al., 2000; Pettegrew et al., 1997; Shonk et al., 1995). Using the decrease in NAA, coupled with the increase in myo-inositol as a simple ratio can sometimes provide better discrimination between treatment groups, or AD vs. controls than use of either metric alone (Choi et al., 2010b; Shonk et al., 1995). In addition to NAA and myo-inositol there are numerous other chemicals that can be measured including glutamate and glutamine, cholines, scyllo-inositol, GABA and taurine that can provide different windows onto the metabolic and pathological processes (Choi et al., 2007). In addition to the use of MRS, there have been great strides in the use of MRI for imaging various brain regions that show degeneration in AD such as hippocampus in both humans (Jack et al., 2012; Sabuncu et al., 2011) and in AD mouse models (Badea et al., 2010; Borg and Chereul, 2008; Redwine et al., 2003) that are correlated with disease progression. Therefore, in this study we used MRS (*in vivo* and *in vitro*) as well as MRI measurements of hippocampal volumes to asses the effects of aging and ibuprofen treatment in a triple transgene model of AD that manifests both Aβ and tau pathology (Oddo et al., 2003).

In addition to the effects of ibuprofen treatment, we also examined the effects of differential housing on the triple transgene animals. There is anecdotal evidence in the community (though not in the literature) that this particular AD model shows more variability than some other AD mouse models. There is good evidence that in a number of transgenic mouse

models differences in housing can lead to different outcomes. Of particular relevance to AD was a paper that showed that anti-nerve growth factor mice raised in pathogen-free conditions, compared to conventional housing, had a significantly delayed onset of neurodegeneration (Capsoni et al., 2012). Thus, we present results here from mice housed in different facilities that demonstrate large differences between the facilities.

Results

We examined the effects of age on the AD temporal cortex using *in vitro* MRS. The data showed a trend for increased myo-inositol with increasing age that was not significant by linear regression ($R = 0.34$; $p>0.1$) or ANOVA ($F_{2,21}= 1.27$; $p<0.3$). There was also a decrease of NAA with age that was significant by linear regression ($R = 0.438$; $p<0.05$) but not ANOVA ($F_{2,21}= 2.36$; $p<0.1$), that is largely driven by the oldest ages. Using the metric myo-inositol/NAA provides additional power to detect changes (linear regression $R = 0.66$; $p<0.001$; $F_{2,21}= 7.35$; $p<0.01$). The increase in effect size, r, calculated from Cohen's d was 0.305, −0.267 to 0.528 for myo-inositol, NAA and myo/NAA respectively. No changes in the creatine concentration were noted as a function of age ($R = 0.18$; $p>0.4$; $F_{2,21}= 0.77$; $p>0.45$). There was also a trend for an increase in the total choline concentration ($R = 0.463$; $p<0.05$; $F_{2,21}= 2.66$; $p<0.1$). These data are shown in Fig. 2.

We switched to HRMAS for the hippocampus and amygdala as it allows for smaller tissue punches to be studied due to the difficulties in the extraction of tiny tissue samples, and the amygdala is quite small. We also examined the caudate/putamen as a control region where pathology is not anticipated using 1 mm punches from the different brain regions as shown in Fig 1. At six months of age the biggest changes were noted in hippocampus. There was a significant increase in myo-inositol in the AD animals that showed some protection by treatment with ibuprofen (i.e. indistinguishable from wild type (WT); Fig. 3). There were no significant changes in other metabolites at this age, compared to WT, when corrected for multiple comparisons, in either the amygdala, hippocampus or striatum. As the age of the mice increased alterations in other metabolites were noted in the hippocampus including increases in aspartate ($p<0.02$), scyllo-inositol ($p<0.001$) and myo-inositol ($p<0.01$). At 23 months of age there were decreases in NAA. In the amygdala the only significant change as a function of age was in myo-inositol which was increased in the mice aged 17–23 months ($p<0.01$). There was a trend to protection at this age with ibuprofen treatment (Fig. 3). In the caudate/putamen there were no significant changes in NAA, however there was an age effect with the levels of myo-inositol showing an increase as a function of age (myo/Cr = 0.57±.05 at 6 months, 0.58±.05 at 15 months and 0.76±0.04 at 23 months; $F_{2,17} = 7.84$; $p = 0.005$).

As discussed in the Experimental Procedures section, we studied a second group of mice housed in a different facility that was subject to total gowning and pathogen protection as well as having individually ventilated cages. These mice showed a similar trend to that noted in Group I with respect to the alterations in the metabolites. In particular, in the hippocampus at 18 months of age we found a decrease in NAA/Cr (WT = 0.73 vs. AD = 0.67; $F_{1,19}= 10.6$; $p<0.01$) and an increase in myo-inositol (WT = 0.63 vs. AD = 0.72; $F_{1,19}= 5.23$; $p<0.05$) using one-way ANOVA. There was an increase in power to detect the

alterations using the myo/NAA ratio that was larger than using either myo-inositol or NAA alone (Cohen's d increases from 0.966 (myo); −1.449 (NAA) to 1.881 (myo/NAA); $F_{1,19}$= 15.2; p = 0.001). Similarly, in the amygdala there were decreases in NAA/Cr (WT = 0.76 vs. AD = 0.71; $F_{1,16}$= 2.94; p = 0.11) and increases in myo-inositol/Cr (WT = 0.56 vs. AD = 0.64; $F_{1,16}$= 5.62; p = 0.035) although the former did not reach significance. Using the myo/NAA ratio increased the power to detect differences (WT = 0.76 vs. AD = 0.90; $F_{1,16}$= 6.57; p = 0.025; Cohen's d increases from −0.929 (NAA); 1.23 (myo) to 1.38 (myo/NAA)).

There were significant differences in the metabolite profiles between the two separately housed groups of mice even though they are the same strain and show similar behavioral and neuropathological deficits to those we previously used (McKee et al., 2008) that were housed in the same facility as the Group I mice. There were significant differences in NAA and GABA levels between the two sets of mice with the mice in the ventilated cages and facility with total gowning requirements showing higher NAA and GABA levels (Table 1). The differences noted between the Group I and Group II mice were larger (either between AD or WT) than the differences between AD and WT within group.

We stained for both tau and Aβ pathology in a subset of the Group I mice. Shown in Fig. 4 are data comparing the effects of ibuprofen treatment in mice 16–23 months old on both tau and Aβ. There was significant protection of the tau pathology, but not the Aβ similar to what we observed earlier ($F_{1,9}$= 7.32; p<0.05; n=5 for regular diet AD and n=5 for ibuprofen (Ibu) treated mice). There was also a trend for smaller Aβ values, that can be anticipated based upon the strong correlation between the PHF-1 and 6E10 values (Fig. 4b) but this was not significant with this relatively small number of mice. There were also significant correlations between some of the MRS metabolite levels and the antibody measurements in the nine mice that were sampled using both techniques. The correlations were strongest for aspartate (p<0.001 and 0.01 for PHF-1 and 6E10 respectively), but were also significant (p<0.05) for glutamate and taurine for PHF-1 and taurine for 6E10.

We also measured *in vivo* MRS in the hippocampus (the voxels are shown in Fig. 5). These measurements were only made in the mice at 20–23 months of age. Similar to the group II animals, these animals were housed in a facility that was pathogen free with total gowning and individually ventilated cages. There was an increase in myo-inositol and a decrease in NAA as measured in the hippocampus compared to the WT animals. The decrease in NAA was protected by the ibuprofen treatment in the sense that the ibuprofen-treated animals showed no significant difference with the WT animals, but were significantly different than the regular diet animals (Fig. 5). The difference between the NAA loss was highly significant with the old regular diet animals showing a 14 and 13% decrease in NAA compared to the WT and Ibu animals respectively (p<0.001 for both). The myo-inositol showed an increase in both the regular and Ibu animals compared to the WT, that was significant ($F_{2,16}$= 4.69; p = 0.03 for the omnibus ANOVA). The regular and Ibu animals did not differ in myo-inositol (p>0.9).

We also measured hippocampal volumes using T2-weighted scans. We measured volumes in age-matched imaging sessions from 17–23 months of age (regular diet, ibuprofen-treated, WT) from the animals housed in the same (MGH) facility. There was a significant decrease

in hippocampal volume between the WT and regular diet animals at this age. The differences between the groups in volume was highly significant (WT = 20.09±.68, Ibu = 18.79±0.63, Regular = 16.52±0.60 mm^3; $F_{2,26} = 7.58$; $p<0.002$) and the difference between the Ibu and WT animals was not significant whereas the difference between the Ibu and regular animals was significant using the Tukey post-hoc comparisons ($p<0.05$). We compared the hippocampal volumes and NAA values for the mice that had both measured (more mice were measured for the hippocampal volumes). There was a correlation that was significant ($p<0.05$) between the two values (Fig. 5).

We compared the ability of simple classifiers based upon metabolites, metabolite ratios and hippocampal volumes to determine the specificity and sensitivity of the tests. The results are shown in Fig. 8 and Table 2 using ROC curves for myo-inositol, NAA and hippocampal volume. We also compared GABA and two different ratios. The first was the myo-inositol/NAA ratio since the chemicals change in opposite directions in the AD animals and our data above showed increased power to detect differences between the groups. We further reasoned that since both myo-inositol and glutamine increase and NAA and GABA decrease that using the ratio of myo*gln/NAA*GABA might provide additional power to classify the animals into AD or WT. The increase in area under the curve was dramatic for this metric (Table 2). These data show the potential value of combining MRS markers to be able to gain additional discriminative power.

Discussion

The triple transgene model has some significant differences with other AD mouse models, most notably it also incorporates mutations in tau that lead to increases in concentrations of hyper-phosphorylated tau in addition to the Aβ deposits (McKee et al., 2008; Oddo et al., 2003; Oddo et al., 2006c). Therefore, it is instructive to compare these data with prior studies from our lab and others of the various AD mouse models.

Comparisons to other AD Mouse Models

We were the first to report MRS findings in AD mice with data from single transgene animals bearing the Swedish mutation in APP (APPTg2576)(Dedeoglu et al., 2004). These mice show many of the pathological features of AD. Older mice also manifested a large decrease in NAA and glutamate and an increase in the osmolar marker taurine, but not, interestingly, myo-inositol. This finding (of increased taurine but not myo-inositol) was subsequently replicated by another lab (Marjanska et al., 2005) that also showed that there was a decrease in NAA and an increase in myo-inositol, but not taurine in a double transgene animal model the PS1×APP. We subsequently confirmed this finding and showed decreases in glutamate and increases glutamine as well in this model (Choi et al., 2010b). We also showed that the NAA loss correlated with plaque density in cortex and that both the plaque burden and NAA levels, but not myo-inositol, were protected by ibuprofen treatment in these mice (Choi et al., 2010b). Another study of the PS1×APP model showed the earliest changes were noted in myo-inositol and not in NAA at 10 months of age (Woo et al., 2010). Another model, the PS2×APP was studied by yet another lab and they showed that there was a very late decrease in NAA in that model and a non-significant increase in myo-inositol in

the frontal cortex (von Kienlin et al., 2005). In that model the plaque burden also correlated with the NAA loss in a similar way to the PS1×APP model (i.e. there appears to be a threshold over about 5% plaque density before the NAA decreases). More recently, two additional models have been studied. One model with only a mutation in tau (rTg4510 - P301L Tau) (Yang et al., 2011) and another with 5 mutations (3 in APP and 2 in PS), the so-called 5×FAD model (Oakley et al., 2006). The former model with only tau mutations shows an age-dependent increase in neurofibrillary tangles and age-dependent hippocampal and cortical neurodegeneration. They show an increase in myo-inositol as well as a decrease in NAA in the hippocampus that was of a large magnitude comparable to that observed in the APPxPS1 and APP mice (Yang et al., 2011). They also show an early increase in gliosis and microglial infiltration characteristic of increased p-tau concentrations. These data suggest that NAA changes are common to both tau and Aβ pathology. The 5×FAD model shows an early increase in Aβ deposition and plaques (Oakley et al., 2006). Interestingly the 5×FAD model shows a decrease in GABA as well as NAA and a smaller increase in myo-inositol (Aytan et al., 2013; Mlynarik et al., 2012). The triple transgene mice reported here show an early increase in myo-inositol in the hippocampus, and a later decrease in NAA. They show a late increase in myo-inositol and decrease in NAA in the cortex. They also show a decrease in GABA at the later ages in hippocampus similar to that reported in the 5×FAD mice (Aytan et al., 2013; Mlynarik et al., 2012) (seeTable 1). There was a later increase in myo-inositol in the amygdala. The amygdala shows a very small decrease in NAA even at very late ages. The caudate-putamen shows a small increase in myo-inositol at late ages.

There are some general principles that can tie together the MRS data from the different mouse models as well as human AD. First, and most importantly all the models show decreased NAA at later stages, although they show onset at different ages. This is consistent with years of studies showing the utility of NAA as a neuronal marker and is also consistent with loss of NAA in human AD reflecting the frank neuronal loss. Our data here show that the NAA loss is greater in cortex than hippocampus, likely because cortex has higher NAA levels at baseline than hippocampus and/or perhaps because the frontal cortex shows earlier staining for extracellular Aβ than does the hippocampus, while the hippocampus shows earlier build-up of tau (Oddo et al. 2003). This remains a fertile question for future studies. We noted a good correlation between *in vivo* NAA levels and hippocampal volumes (Fig. 7e). Since hippocampal volumes are a good predictor of progression from MCI to AD in humans this supports the use of NAA as an additional marker. However, our data, as well as those we have previously published show additional statistical power is obtained using combined markers (see Fig. 8) – which may be the best way to use MRS in clinical trials of human AD. Second, while a number of models, including the triple transgene mice here, show increased myo-inostiol, not all models do. For instance the increase in myo-inositol seems to be replaced by an increase in taurine in the APP model (Dedeoglu et al., 2004). Since both taurine and myo-inostiol have much higher concentrations in glial cells than neurons this suggests that subtle differences in glial cell metabolism may dictate whether myo-inositol or taurine concentrations are upregulated. Humans, have much less taurine than rodents, and may therefore show the elevated myo-inositol (Choi et al. 2010).

Effects of Housing

We unexpectedly discovered a profound effect of housing on the neurochemical profile of the triple transgene animals that similarly affected the WT and transgene animals (Table I). Unfortunately, we did not plan this as a variable to be investigated in the study so the conclusions to be drawn are preliminary. However, given the anecdotal observations that there is some variability in this mouse model (though these are not published) we thought it worth quantifying. In the hippocampus we noted a decrease in GABA that was significant in the second group of animals scanned (Group II), similar to what is noted in the 5×FAD animals (Aytan et al. 2013; Mlynarik et al., 2012). The GABA levels were much higher in the Group II WT animals vs. the Group I WT animals (0.48 vs. 0.30, $p < 0.001$; Table I) suggesting that the GABA levels in the Group I animals were already as low as might be possible before the onset of AD symptoms. Group I mice also showed a very significant difference in the NAA levels (0.61 vs. 0.46, $p<0.001$; Table I). This group also showed no decrease in NAA in the AD animals in contrast with the Group II animals or the *in vivo* MRS animals, both of which showed large (15%) decreases in NAA, again implying there is a “floor” level below which NAA does not drop. Very early studies of the species dependence of NAA concentrations from the 1950’s showed that different strains of mice could readily vary by factors of two or more (see review in (Birken and Oldendorf, 1989)). This contrasts with humans where NAA levels from similar brain regions show much less variability. This issue of differing housing requires further verification and study, however it is clear that there can be very large differences between the same strain of mice housed in very different facilities. Both the Group II and *in vivo* MRS animals were housed in facilities that had full gowning and changing rooms (which are entered prior to going into the animal cage rooms) as well as individually ventilated cages. Both the *in vitro* and *in vivo* MRS showed that the Group II and *in vivo* animals had similarly high NAA values. We have previously shown excellent correlations between *in vivo* and *in vitro* measures of NAA in rat models of neurodegeneration (Jenkins et al., 1996), mouse models of Huntington’s disease (Chen et al., 2005; Ferrante et al., 2000), amyotrophic lateral sclerosis (Carreras et al., 2010), and AD (Carreras et al., 2010). The facility where the Group I animals were housed was older and not subject (at the time of the data collection) to total gowning nor did it have individually ventilated cages. This suggests that comparisons between animals housed in different facilities needs to be made carefully.

A similar finding has been made with mice deficient in nerve growth factor where pathogen-free housing delayed onset of the neurodegeneration noted in that model (Capsoni et al., 2012). Similar issues have arisen when comparing non-obese mouse models of diabetes (Pozzilli et al., 1993; Wen et al., 2008) where different levels of bacteria in housing facilities can dramatically alter the incidence of type I diabetes. In spite of the differences between the groups, the overall pattern of increased myo-inositol was preserved in the three groups of animals while the NAA loss was observed in the two groups of animals (for both *in vivo* and *in vitro* studies) with individually ventilated cages and was observed in the cortex for the group I animals. Clearly this issue warrants more study.

Effects of Ibuprofen Treatment

We previously studied the PS1×APP model using ibuprofen treatment. The ibuprofen showed protection of both plaque density and Aβ42 (measured using ELISA) in that model. We also showed that the ibuprofen protected against the NAA loss at 18 months of age, but had no effect on myo-inositol at that age (Choi et al., 2010b). Similarly in this study we found protection of the NAA loss at older ages in the hippocampus and no effect of ibuprofen on myo-inositol. We did, however, find that the myo-inositol increase seen in the regular diet animals was protected in the ibuprofen-treated animals at 6–7 month of age in the hippocampus as shown in Fig. 4. There is evidence suggesting that Aβ moves from being intracellular at young ages to appearing extra-cellularin older mice in this mouse model (Mastrangelo and Bowers, 2008; Oddo et al., 2006a; Oddo et al., 2006b), and the tau pathology follows after Aβ becomes extracellular. Oddo et al. (Oddo et al., 2003) found in these triple transgene mice, that the Aβ immune reactivity was first detected intraneuronally and later in extracellular locations in the cortex. Since we found that ibuprofen protects against NAA loss in this model and in the PS1×APP mice (Fig. 6 and (Choi et al., 2010b)), and since NAA is also an intracellular marker, it may be that ibuprofen, somewhat paradoxically, has little effect on extracellular pathology. This is supported by the data in these mice showing protection against tau, but not the neuritic plaques (Fig. 5). This concept is also supported by our prior data in these mice where we found protection against Aβ pathology at young ages (6 months) when the Aβ is mostly intraneuronal (McKee et al. 2008). We also found a reasonably good correlation between NAA and hippocampal volume (Fig. 7), suggesting that these two metrics are related and the hippocampal volume decrease seen in these mice was protected with ibuprofen. The latter fact suggests the hippocampal volume decrease may be related to the tau pathology and not Aβ pathology. Recent studies using the Alzheimer's disease neuroimaging initiative (ADNI) data have found that total hippocampal volume loss correlates well with CSF tau and not as well with Aβ (Carmichael et al., 2012).

Prior studies with ibuprofen have produced ambiguous results with different mouse models. This is likely due to the dual effects of the drug as both an anti-inflammatory as well as an inhibitor of γ-secretase as well as the different ages of mice investigated. For instance, in the 5×FAD model with a pre-senilin mutation that renders it resistant to γ-secretase modulation, ibuprofen produced decreased inflammation but had no effect on Aβ plaque accumulation (Hillmann et al., 2012). As discussed above, our prior studies of PS1×APP mice showed protection against Aβ plaque deposition, but the data here show only protection against tau pathology as we have also recently shown in another study of the triple transgene animals using the NSAID flurbiprofen as a treatment (Carreras et al., 2013). Older studies in the APP Swedish mutation mouse model showed large decreases in Aβ plaque accumulation with ibuprofen treatment (Lim et al., 2000; Lim et al., 2001). This was also found in PS1×APP mice but in that model the decrease in Aβ was restricted to non-fibrillar deposits (Jantzen et al., 2002) again, consistent with protective effects acting intra-cellularly. Thus, it is clear that there is mixed evidence for the efficacy of ibuprofen. This parallels what has been observed in humans where epidemiologic retrospective studies show that ibuprofen can protect against development of AD, but prospective studies of ibuprofen treatment, as well as numerous other NSAIDs in mild AD have been negative (Jaturapatporn et al., 2012).

Experimental Procedures

Mice and treatment

Homozygous 3×Tg-AD mice expressing mutant human genes APP_{swe}, $PS1_{M146V}$ and tau_{P301L}, previously characterized by Oddo et al., (Oddo et al., 2003) and wild-type (WT) mice from the same hybrid background strain, 129/C57BL6, were used in the study. Three separate groups of mice were studied, two for *in vitro* studies and a third for *in vivo* studies. The mice were studied at roughly three time points: 5–7 months of age, 12–14 months of age, and 17–23 months of age. Ibuprofen (Sigma, 375 ppm) was formulated into animal diets (Research Diets Inc., NJ, USA) and groups were treated with either normal chow or the ibuprofen-treated chow starting from one month of age. Mice were monitored for general well being and had weekly body weights and daily food consumption measured. The WT mice were not treated with ibuprofen. During the course of the study, the laboratory housing the mice was moved from the Bedford VA Medical Center to the Boston VA Medical Center. The Bedford facility was not subject to total gowning procedures before humans could enter the facility nor were the individual cages housing the mice ventilated. These animals were labeled as Group I. Another group of mice from the Boston VA Medical Center was studied and this was labeled Group II. A third group of mice for the *in vivo* MRS and MRI were housed at the MGH facility, also in Boston. The latter two housing facilities were subject to total gowning procedures and both have individually ventilated cages. There were no differences in the number of animals housed per cage (5/cage) at the three facilities.

To collect samples for MRS mice were euthanized under using CO_2 under isoflurane anesthetic. The brain was immediately dissected coronally. For *in vitro* MRS, tissue punches were taken from the left hemisphere in the hippocampus (subiculum), amygdala and striatum. Tissue punches were 1.2 mm in diameter and were immediately placed into Eppendorf tubes sitting on dry ice and were then transferred to a −80°C freezer until they were run on the spectrometer.

We additionally studied cortical tissue dissected in the manner described above except that the tissue was extracted from temporal cortex.

All animal studies were approved by the Institutional Animal Care and Use Committee (IACUC) and in accordance with the NIH Guide for the Care and Use of Laboratory Animals.

Magnetic Resonance Spectroscopy and Imaging

In vitro MRS was collected as previously published (Carreras et al., 2010; Choi et al., 2010a; Dedeoglu et al., 2004). For the hippocampus and amygdala, we collected high resolution magic angle spinning (HRMAS) spectra on Bruker 14T (Billerica, MA). We obtained tissue punches of freshly frozen hippocampus from mice. The dissected tissue sample was placed into a glass cylinder positioned in a 3 mm zirconium oxide MAS rotor (volume 50μL). HRMAS measurements were performed using a sample spinning rate, of 3.6 kHz selected to push the spinning side bands outside the frequency region of the metabolites. The experiments were performed at 4°C to minimize tissue degradation.

Data were acquired using a rotor synchronized, T_2-filtered Carr–Purcell–Meiboom–Gill (CPMG) pulse sequence [90 − (τ− 180 −τ)$_n$− Acq] with two different effective TEs (100ms/10ms). The longer TE serves to remove the lipid/macromolecular resonances and the short TE retains them. The interpulse delay, τ, is synchronized to the rotor frequency, and is 272μs. The n value for the relatively short T_2 filter was 36 and for the long TE was 360. The short τ value removes all the T_2* - like effects on the lineshapes. The long T_2 filter yields approximately 95% of the total spectral intensity of all metabolites of interest compared to the short TE. Other acquisition parameters were a 90° pulse of 5–10 μs, a spectral width of 8 kHz, 16K complex points, 256 averages and a TR of 5s. Samples were placed in the rotor with a small amount of D_2O (Sigma-Aldrich, Milwaukee, WI) for locking and shimming.

Brain extract data were also run from cortex at 600 MHz using a simple one-pulse experiment (TR 12s; 16K points; 0.139ms acquisition time) in D_2O with suppression of residual water. Absolute concentration measurements were made using an internal standard (DSS; 0.5 mM) as previously described (Carreras et al., 2010; Choi et al., 2010a; Dedeoglu et al., 2004). Concentrations are reported as micromoles/gram of tissue wet weight.

Data were analyzed using the Chenomx (Edmonton, Alberta, Canada) package fitting the entire metabolite spectrum for each neurochemical. HRMAS data were reported as molar ratios to creatine since our prior studies of the absolute concentrations in multiple different AD transgenic mouse models showed no change in total creatine between WT and any of the AD models (Carreras et al., 2010; Choi et al., 2010a; Dedeoglu et al., 2004).

In vivo MRS data were collected in older mice (20–23 months of age) as described previously (Carreras et al., 2010; Choi et al., 2010a; Jenkins et al., 2000; Jenkins et al., 2005). Mice were placed in a home-built head holder and anesthetized using isoflurane/O_2/air (1.2%/70/30). Images were acquired with a 1.5cm transmit receive surface coil place down over the mouse's head. MRS was collected using a PRESS sequence localized to the hippocampus with an average voxel size of 2.45±.05× 1.36±.06 × 1.8mm with a TR of 2200ms and spectra with TEs of 15 and 136 ms. The voxel size varied slightly in the x and y dimensions with the reasoning that there would be less variability by tailoring the voxel to the hippocampal size rather than including more partial volume averaging with a uniform voxel size due to the different sizes of the hippocampi. The MRS voxel was prescribed from the T2 images collected immediately before the MRS. The data were analyzed using fitting of the total metabolite spectrum with basis metabolites in the jMRUI package (Decanniere et al.) with the QUEST fitting routine (Decanniere et al.) using simulated metabolite files generated using the GAMMA package. *In vivo* data were analyzed for NAA, glutamate, glutamine, creatine, total choline, taurine and myo-inositol.

MR Imaging was collected using a T2-weighted RARE sequence with 0.12 mm in plane spatial resolution and 0.5mm slices in mice 17–23 months of age. The brains were analyzed using manual segmentation of the hippocampus as shown in Fig. 1. The *in vivo* MRS and MRI data were run in either age-matched pairs or triples (WT; IBU; Reg) randomly selected from their cages and run in random order on the day of the scan.

All the MRS data and MRI data were analyzed with the data analyst blinded to the type of mouse. To ensure this all files were stored with codes that did not indicate the animal type. After the data were analyzed (i.e. the MRS quantification and the hippocampal volumes) the blinds were broken. The *in vitro* MRS was run with 4–6 samples per scan session, also in age-matched and group matched (e.g. WT, regular diet, ibuprofen) combinations.The use of the creatine as the denominator for the HRMAS and *in vivo* MRS data controls for any potential CSF contamination in the MRS results since CSF has no MRS measureable neurochemicals.

Post Mortem Histological Data

A subset of the mice from Group I were stained for anti-bodies that reflect tau pathology (PHF-1) or A-beta accumulation (6E10). Immediately after mice were euthanized by CO_2 asphyxiation, the brains were removed. The right hemi-brains, from the same mice that were dissected for HRMAS above, were cut into 3 coronal sections, 2 mm in thickness, using a coronal matrix. The 3 coronal sections, which spanned from 3 mm anterior to the bregma to 3 mm posterior to the bregma, were fixed in 4% paraformaldehyde at room temperature for 2 hours and embedded in a single paraffin block. The paraffin-blocks were cut serially in 10 μm sections, each section consisted of 3 anterior-posterior coronal levels and each block encompassed the entire mid section of the hemi-brain. Sections were immunostained using the following antibodies: 6E10 (Signet Laboratories, 1:1000 dilution, pretreated with formic acid) which is reactive to amino acid residue 1–16 of beta amyloid, and PHF-1, directed against phosphoserine 396 and phosphoserine 404 (courtesy of P. Davies, 1:1000). Sections for immunostaining were processed using the Vectastain Elite ABC Kit (Vector Labs, Burlingame, CA). Following the appropriate biotinylated secondary antibody, slides were developed with diaminobenzidine (DAB) for the exact same amount of time and counterstained with hematoxylin. For double immunostained sections, the tissue was blocked with avidin and biotin before each primary antibody (Multiple Antigen Labeling, Vector Labs). The first primary antibody was visualized with DAB, the second primary antibody was visualized with aminoethylcarbazole.

To quantify Aβ and Tau immunoreactivity we measured optical density. Stained histological sections were analyzed by taking digital images with Nikon Eclipse 80i microscope using an Optronics camera. Quantification of immunoreactivity in the subiculum area of the hippocampus was performed blindly using a house-written Matlab program that processes JPEG pictures of the region of interest and creates black and white images to provide percent immunoreactivity. Each image was normalized for color and brightness using an unaffected region of the section. The percentage of thresholded pixels to total pixels in the region of interest was calculated for each image and presented as the percentage of affected tissue in the subiculum.

Statistical Analysis

All data were analyzed using one-way (with respect to age or drug treatment, or housing) ANOVA with post-hoc analyses using the Tukey HSD. We did not use two-way ANOVAs (e.g. incorporating brain region as a factor) since the brain regions vary widely in neurochemical levels in the WT animals. We also performed simple linear regression

analyses for the effects of age. Receiver operator characteristic (ROC) curves were created to examine the ability of simple thresholds using neurochemical levels and hippocampal volumes to classify the animals into AD or WT. For all the data animal numbers are indicated in the text, figures and/or tables for the specific experiments.

For all figures in the text a * represents $p<0.05$; ** $p< 0.01$; *** $p < 0.001$.

Acknowledgement

This research is supported by Grants from NIA (R01AG031896) to A. Dedeoglu and the Department of Veteran Affairs (Merit Award) to A. Dedeoglu.

References

Aytan N, et al. Combination therapy in a transgenic model of Alzheimer's disease. Exp Neurol. 2013; 250C:228–238. [PubMed: 24120437]

Badea A, Johnson GA, Jankowsky JL. Remote sites of structural atrophy predict later amyloid formation in a mouse model of Alzheimer's disease. Neuroimage. 2010; 50:416–427. [PubMed: 20035883]

Birken DL, Oldendorf WH. N-Acetyl-L-Aspartic Acid: A Literature Review of a Compound Prominent in 1H-NMR Spectroscopic Studies of Brain. Neurosci. Biobehavior. Rev. 1989; 13:23–31.

Borg J, Chereul E. Differential MRI patterns of brain atrophy in double or single transgenic mice for APP and/or SOD. J Neurosci Res. 2008; 86:3275–3284. [PubMed: 18646206]

Capsoni S, Carucci NM, Cattaneo A. Pathogen free conditions slow the onset of neurodegeneration in a mouse model of nerve growth factor deprivation. J Alzheimers Dis. 2012; 31:1–6. [PubMed: 22504318]

Carmichael O, et al. Localized hippocampus measures are associated with Alzheimer pathology and cognition independent of total hippocampal volume. Neurobiol Aging. 2012; 33:1124, e31–e41. [PubMed: 22169204]

Carreras I, et al. Moderate exercise delays the motor performance decline in a transgenic model of ALS. Brain Res. 2010; 1313:192–201. [PubMed: 19968977]

Carreras I, et al. R-flurbiprofen improves tau, but not Ass pathology in a triple transgenic model of Alzheimer's disease. Brain Res. 2013; 1541:115–127. [PubMed: 24161403]

Chen YC, et al. Mapping dopamine D2/D3 receptor function using pharmacological magnetic resonance imaging. Psychopharmacology (Berl). 2005; 180:705–715. [PubMed: 15536545]

Choi JK, Dedeoglu A, Jenkins BG. Application of MRS to mouse models of neurodegenerative illness. NMR Biomed. 2007; 20:216–237. [PubMed: 17451183]

Choi JK, et al. Detection of increased scyllo-inositol in brain with magnetic resonance spectroscopy after dietary supplementation in Alzheimer's disease mouse models. Neuropharmacology. 2010a; 59:353–357. [PubMed: 20399219]

Choi JK, et al. Anti-inflammatory treatment in AD mice protects against neuronal pathology. Exp Neurol. 2010b; 223:377–384. [PubMed: 19679126]

Decanniere C, et al. Correlation of rapid changes in the average water diffusion constant and the concentrations of lactate and ATP breakdown products during global ischemia in cat brain. Magn Reson Med. 1995; 34:343–352. [PubMed: 7500873]

Dedeoglu A, et al. Magnetic resonance spectroscopic analysis of Alzheimer's disease mouse brain that express mutant human APP shows altered neurochemical profile. Brain Res. 2004; 1012:60–65. [PubMed: 15158161]

Ferrante RJ, et al. Neuroprotective effects of creatine in a transgenic mouse model of Huntington's disease. J Neurosci. 2000; 20:4389–4397. [PubMed: 10844007]

Hillmann A, et al. No improvement after chronic ibuprofen treatment in the 5XFAD mouse model of Alzheimer's disease. Neurobiol Aging. 2012; 33:833, e39–e50. [PubMed: 21943956]

in t' Veld BA, et al. Nonsteroidal antiinflammatory drugs and the risk of Alzheimer's disease. N Engl J Med. 2001; 345:1515–1521. [PubMed: 11794217]

Jack CR Jr. Alzheimer disease: new concepts on its neurobiology and the clinical role imaging will play. Radiology. 2012; 263:344–361. [PubMed: 22517954]

Jack CR Jr, et al. Shapes of the trajectories of 5 major biomarkers of Alzheimer disease. Arch Neurol. 2012; 69:856–867. [PubMed: 22409939]

Jantzen PT, et al. Microglial activation and beta-amyloid deposit reduction caused by a nitric oxide-releasing nonsteroidal anti-inflammatory drug in amyloid precursor protein plus presenilin-1 transgenic mice. J Neurosci. 2002; 22:2246–2254. [PubMed: 11896164]

Jaturapatporn D, et al. Aspirin, steroidal and non-steroidal anti-inflammatory drugs for the treatment of Alzheimer's disease. Cochrane Database Syst Rev. 2012; 2:CD006378. [PubMed: 22336816]

Jenkins B, et al. Non-Invasive neurochemical analysis of focal excitotoxic lesions iin models of neurodegenerative illness using spectroscopic imaging. J. Cereb. Blood Flow Metab. 1996; 16:450–461. [PubMed: 8621749]

Jenkins BG, et al. Nonlinear decrease over time in N-acetyl aspartate levels in the absence of neuronal loss and increases in glutamine and glucose in transgenic Huntington's disease mice. J Neurochem. 2000; 74:2108–2119. [PubMed: 10800956]

Jenkins BG, et al. Effects of CAG repeat length, HTT protein length and protein context on cerebral metabolism measured using magnetic resonance spectroscopy in transgenic mouse models of Huntington's disease. J Neurochem. 2005; 95:553–562. [PubMed: 16135087]

Johnson KA, et al. Brain imaging in Alzheimer disease. Cold Spring Harb Perspect Med. 2012; 2:a006213. [PubMed: 22474610]

Kantarci K, et al. Regional metabolic patterns in mild cognitive impairment and Alzheimer's disease: A 1H MRS study. Neurology. 2000; 55:210–217. [PubMed: 10908893]

Lim GP, et al. Ibuprofen suppresses plaque pathology and inflammation in a mouse model for Alzheimer's disease. J Neurosci. 2000; 20:5709–5714. [PubMed: 10908610]

Lim GP, et al. Ibuprofen effects on Alzheimer pathology and open field activity in APPsw transgenic mice. Neurobiol Aging. 2001; 22:983–991. [PubMed: 11755007]

Marjanska M, et al. Monitoring disease progression in transgenic mouse models of Alzheimer's disease with proton magnetic resonance spectroscopy. Proc Natl Acad Sci U S A. 2005; 102:11906–11910. [PubMed: 16091461]

Mastrangelo MA, Bowers WJ. Detailed immunohistochemical characterization of temporal and spatial progression of Alzheimer's disease-related pathologies in male triple-transgenic mice. BMC Neurosci. 2008; 9:81. [PubMed: 18700006]

McGeer PL, McGeer EG. NSAIDs and Alzheimer disease: Epidemiological, animal model and clinical studies. Neurobiol Aging. 2007; 28:639–647. [PubMed: 16697488]

McKee AC, et al. Ibuprofen reduces Abeta, hyperphosphorylated tau and memory deficits in Alzheimer mice. Brain Res. 2008; 1207:225–236. [PubMed: 18374906]

Mlynarik V, et al. Proton and phosphorus magnetic resonance spectroscopy of a mouse model of Alzheimer's disease. J Alzheimers Dis. 2012; 31(Suppl 3):S87–S99. [PubMed: 22451319]

Mullane K, Williams M. Alzheimer's therapeutics: continued clinical failures question the validity of the amyloid hypothesis-but what lies beyond? Biochem Pharmacol. 2013; 85:289–305. [PubMed: 23178653]

Oakley H, et al. Intraneuronal beta-amyloid aggregates, neurodegeneration, and neuron loss in transgenic mice with five familial Alzheimer's disease mutations: potential factors in amyloid plaque formation. J Neurosci. 2006; 26:10129–10140. [PubMed: 17021169]

Oddo S, et al. Triple-transgenic model of Alzheimer's disease with plaques and tangles: intracellular Abeta and synaptic dysfunction. Neuron. 2003; 39:409–421. [PubMed: 12895417]

Oddo S, et al. A dynamic relationship between intracellular and extracellular pools of Abeta. Am J Pathol. 2006a; 168:184–194. [PubMed: 16400022]

Oddo S, et al. Temporal profile of amyloid-beta (Abeta) oligomerization in an in vivo model of Alzheimer disease. A link between Abeta and tau pathology. J Biol Chem. 2006b; 281:1599–1604. [PubMed: 16282321]

Oddo S, et al. Reduction of soluble Abeta and tau, but not soluble Abeta alone, ameliorates cognitive decline in transgenic mice with plaques and tangles. J Biol Chem. 2006c

Pettegrew JW, et al. Magnetic resonance spectroscopic changes in Alzheimer's disease. Ann N Y Acad Sci. 1997; 826:282–306. [PubMed: 9329700]

Pozzilli P, et al. NOD mouse colonies around the world--recent facts and figures. Immunol Today. 1993; 14:193–196. [PubMed: 8517916]

Redwine JM, et al. Dentate gyrus volume is reduced before onset of plaque formation in PDAPP mice: a magnetic resonance microscopy and stereologic analysis. Proc Natl Acad Sci U S A. 2003; 100:1381–1386. [PubMed: 12552120]

Sabuncu MR, et al. The dynamics of cortical and hippocampal atrophy in Alzheimer disease. Arch Neurol. 2011; 68:1040–1048. [PubMed: 21825241]

Shonk TK, et al. Probable Alzheimer disease: diagnosis with proton MR spectroscopy. Radiology. 1995; 195:65–72. [see comments]. [PubMed: 7892497]

Stewart WF, et al. Risk of Alzheimer's disease and duration of NSAID use. Neurology. 1997; 48:626–632. [PubMed: 9065537]

von Kienlin M, et al. Altered metabolic profile in the frontal cortex of PS2APP transgenic mice, monitored throughout their life span. Neurobiol Dis. 2005; 18:32–39. [PubMed: 15649694]

Wen L, et al. Innate immunity and intestinal microbiota in the development of Type 1 diabetes. Nature. 2008; 455:1109–1113. [PubMed: 18806780]

Westman E, et al. Combining MRI and MRS to distinguish between Alzheimer's disease and healthy controls. J Alzheimers Dis. 2010; 22:171–181. [PubMed: 20847449]

Woo DC, et al. Regional metabolic alteration of Alzheimer's disease in mouse brain expressing mutant human APP-PS1 by 1H HR-MAS. Behav Brain Res. 2010; 211:125–131. [PubMed: 20307581]

Yang D, et al. Volumetric MRI and MRS provide sensitive measures of Alzheimer's disease neuropathology in inducible Tau transgenic mice (rTg4510). Neuroimage. 2011; 54:2652–2658. [PubMed: 21035554]

Highlights

1. Ibuprofen protects hippocampal volume and NAA loss in triple transgene AD mice.
2. Strong correlations are noted between hippocampal volumes and NAA levels.
3. APP×PS1×Tau mice, unlike APPxPS1 mice show decreased GABA levels.
4. Housing has a strong influence on baseline neurochemical parameters of these mice.
5. Tau, but not A-beta levels are protected in APP×PS1×Tau mice with ibuprofen.

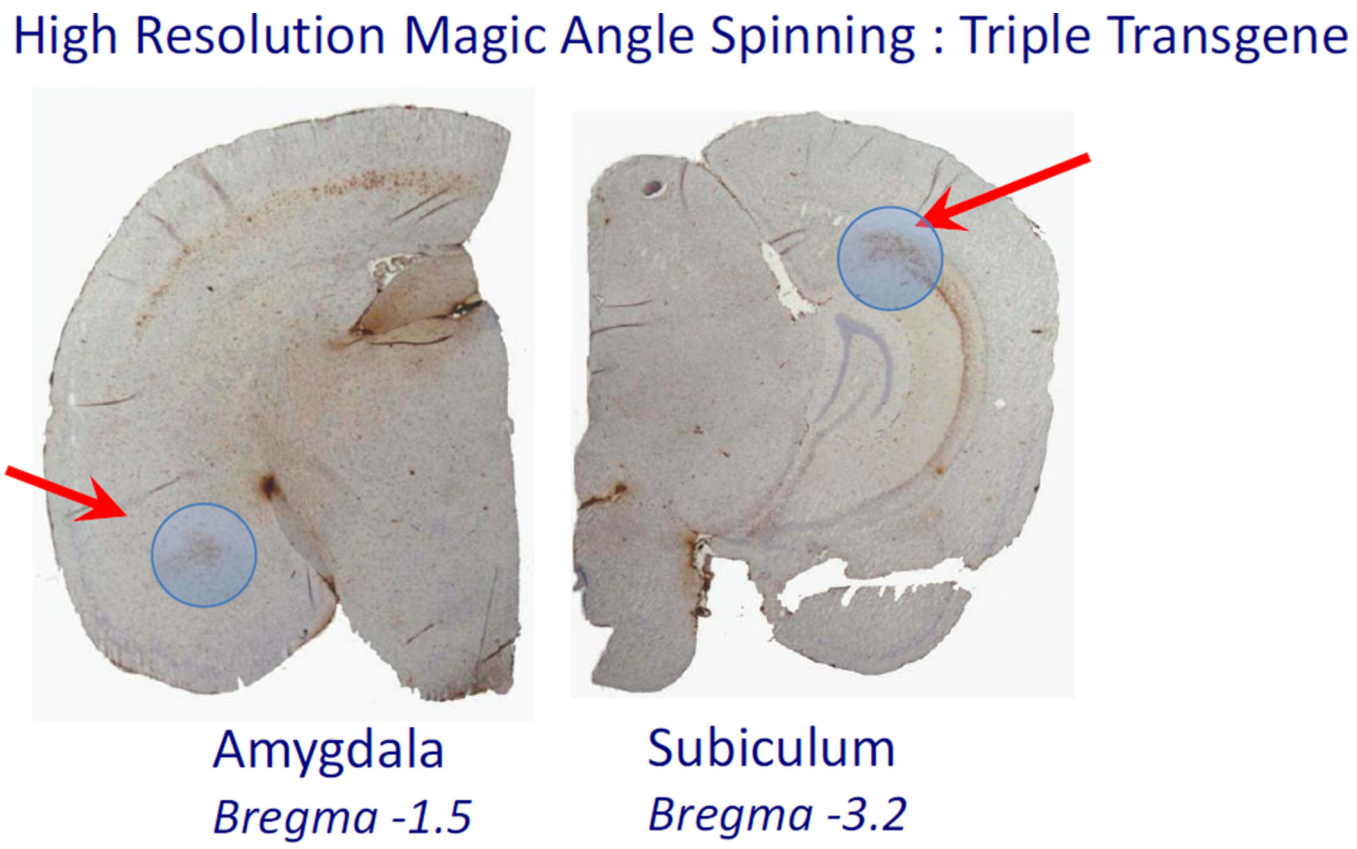

Figure 1.

Picture of a post-mortem 3×Tg brain with blue circles indicating the punches from amydala and subiculum area of the hippocampus. The brain is stained with 6E10 antibody showing the pattern of accumulation in the brain.

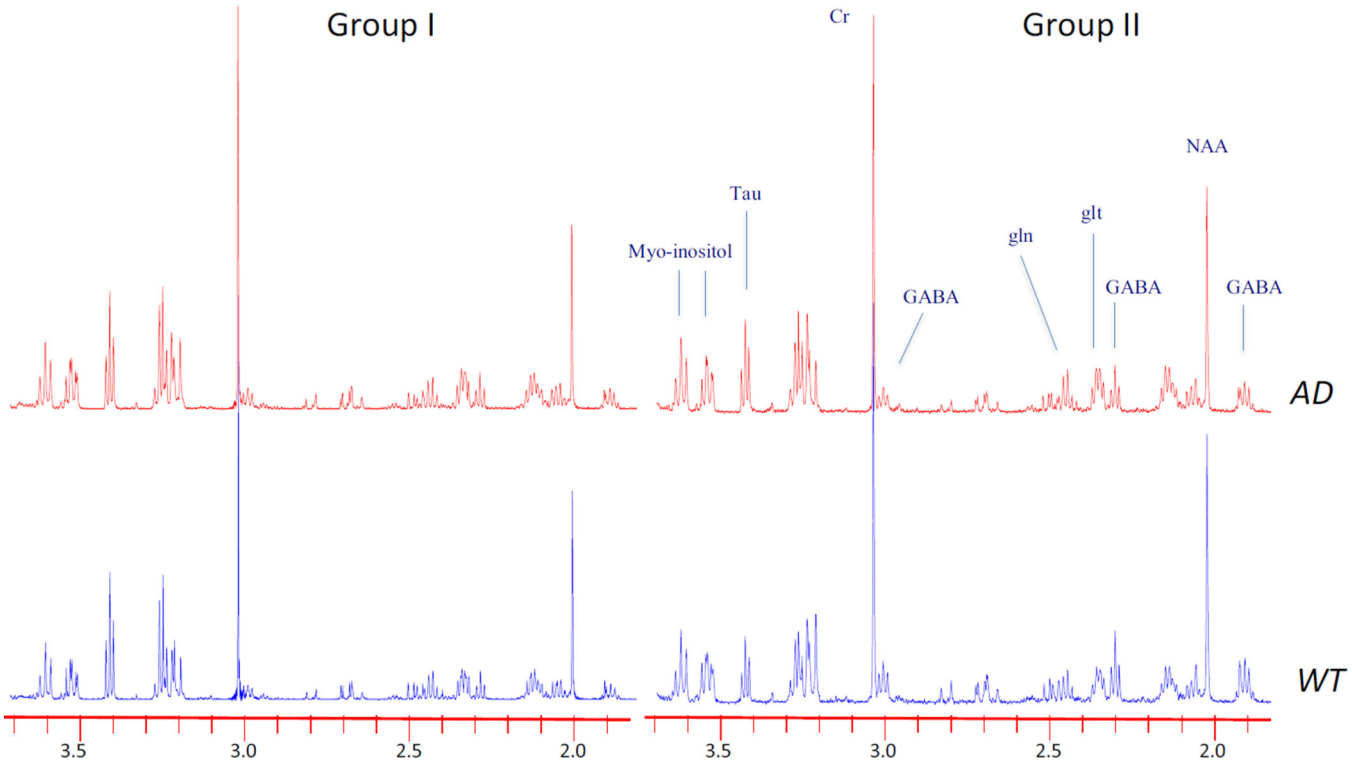

Figure 2.

Effects of housing on neurochemicals in 3×Tg animals. Plots of representative ^{1}H HRMAS spectra from hippocampus in the Group I and Group II animals for both WT and transgene animals. The NAA and GABA are lower in the Group I mice than in the Group II mice – even in the WT. Both groups of AD mice show increased myo-inositol. Plots are scaled such that the Cr resonance at 3 ppm is the same in all spectra.

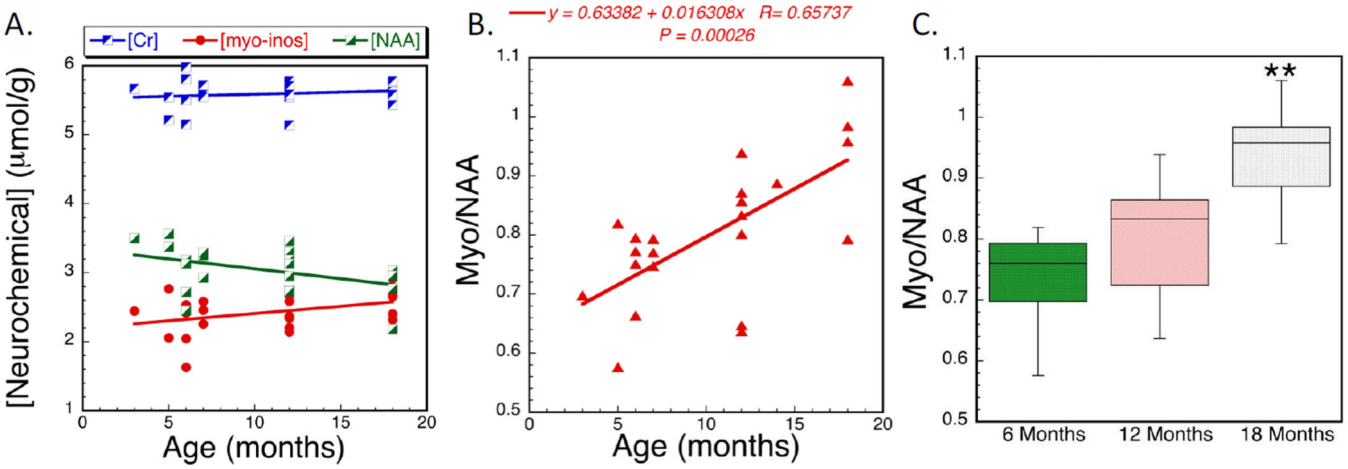

Figure 3.

Neurochemical changes in cortex of Group I mice. The data represent absolute concentrations from brain extracts showing A) no changes in creatine as a function of age, whereas NAA decreases and myo-inositol increases as a function of age. Using the myo-inositol/NAA ratio shows greater power to detect the changes by both linear regression (B) and using an ANOVA ($F_{2,21}$= 7.35; p<0.01 for the effects of age). Data in (C) are plotted as a box plot.

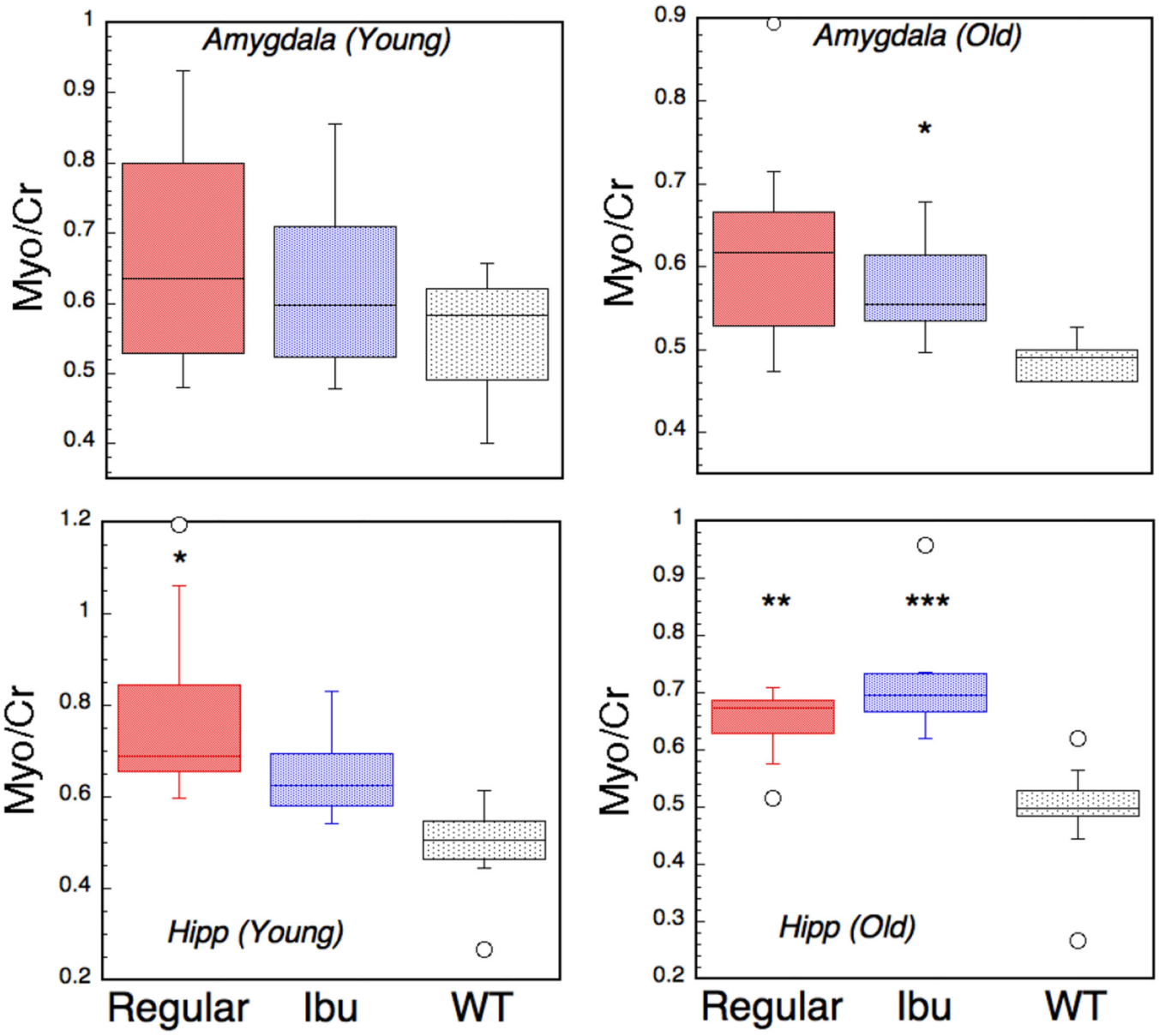

Figure 4.

Box plots of increases in myo-inositol in amygdala and hippocampus (hipp) as measured using ^{1}H HRMAS in young mice (6–7 months of age) and in older mice (17–22 months). There is a significant change in myo-inositol in the young mice in hippocampus but not amygdala. The ibuprofen shows protection of the increase in myo-inositol at a time when the Aβ is mostly intracellular. At the older ages there is an increase in myo-inositol in the hippocampus that is not protected by ibuprofen treatment.

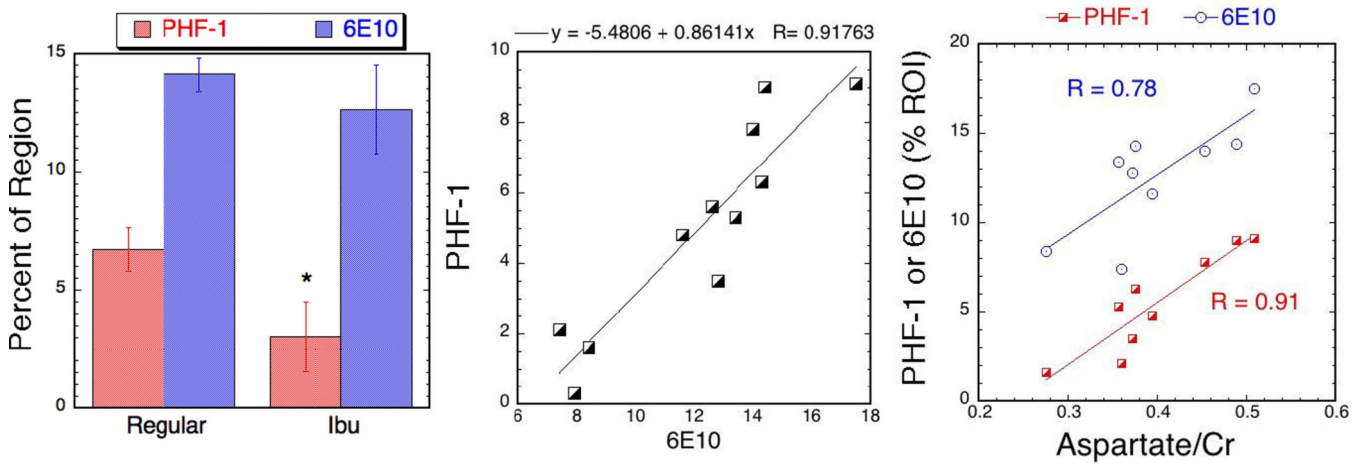

Figure 5.

Effects of ibuprofen treatment on Aβ (6E10 staining) and tau (PHF-1 staining) pathology in the hippocampus. There is a significant protection of the tau pathology as shown in (A) ($F_{1,9}$ =7,32; $p<0.05$). There was also a trend for smaller Aβ values, that can be anticipated based upon the strong correlation between the PHF-1 and 6E10 values (B) but this was not significant. A number of neurochemicals showed strong correlations with the tau and Aβ pathology that was strongest for aspartate.

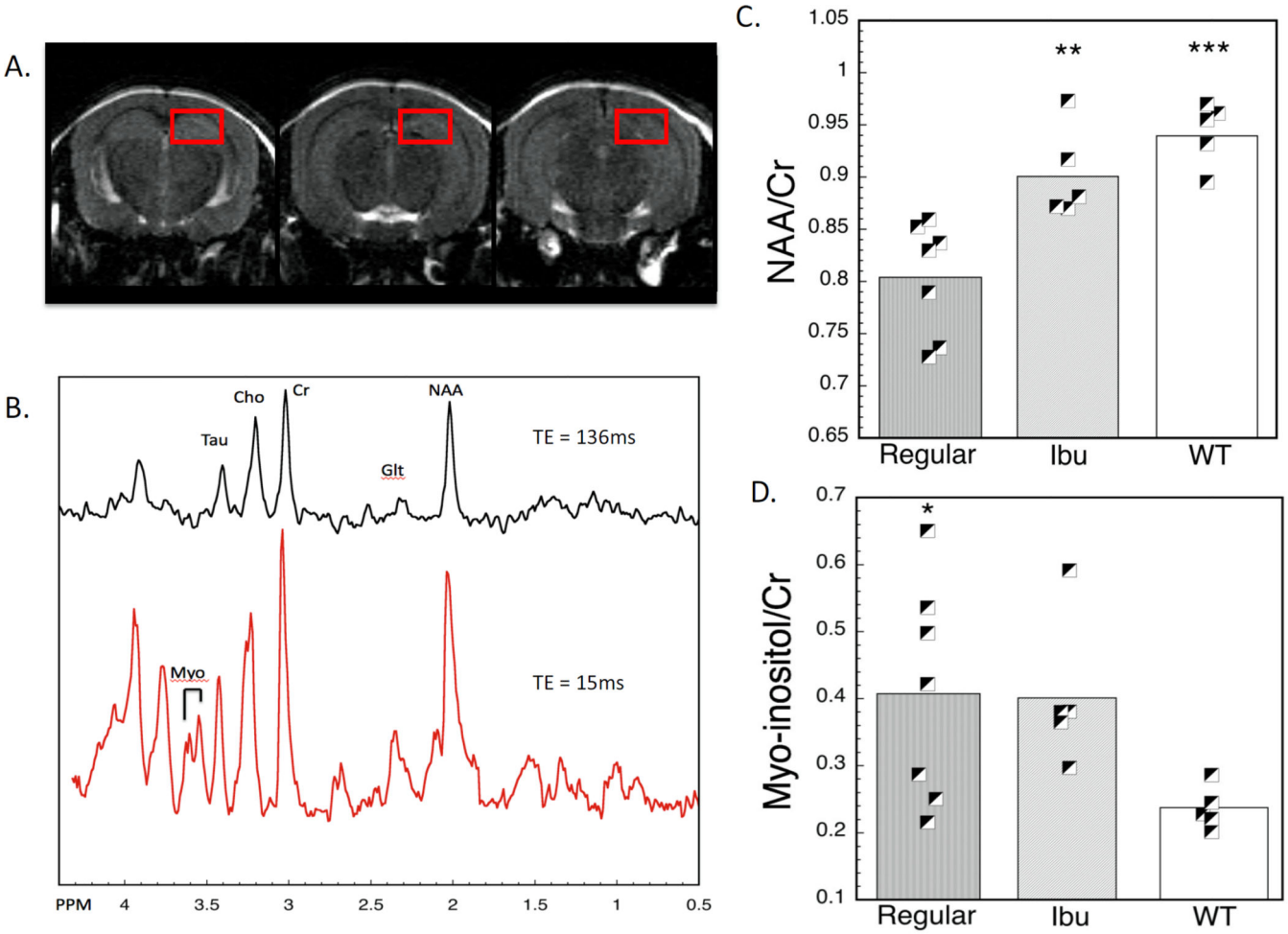

Figure 6.

In vivo MRS and effects of ibuprofen treatment.(A) Images with the voxels used for the hippocampal MRS. (B) Typical MRS spectrum of a aged 3×Tg mouse at two echo times. (C) Plot of NAA/Cr levels as a function of ibuprofen treatment. Both the ibuprofen and WT values are significantly higher than the regular diet animals. (D) Plot of myo-inositol/Cr levels as a function of ibuprofen treatment. In these aged mice there were no protective effects of ibuprofen on myo-inositol.

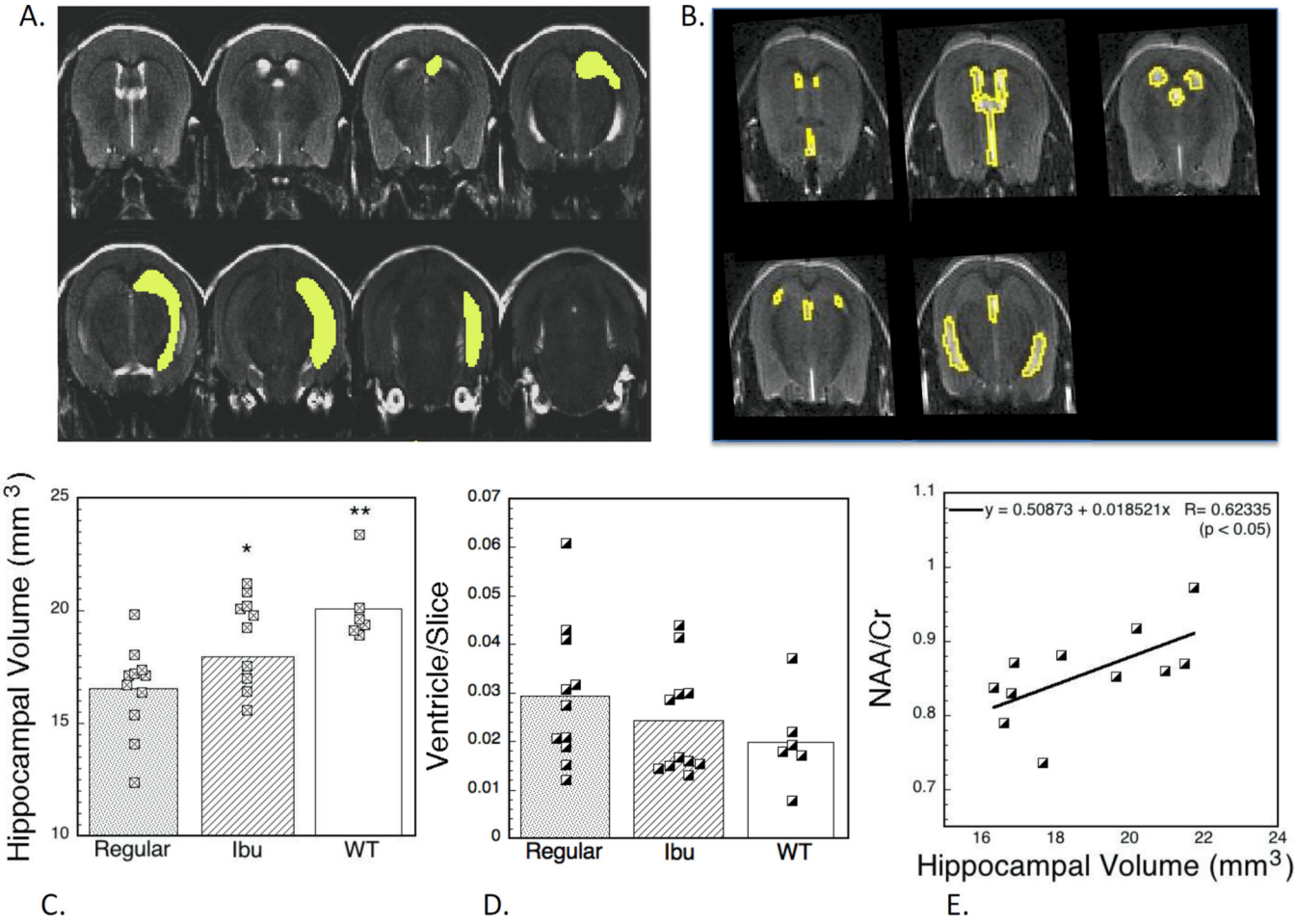

Figure 7.

In vivo MRI and effects of ibuprofen treatment. (A) T2-weighted image showing the manual segmentation of the hippocampus used, as well as the segmentation of the ventricles (B). (C) Absolute hippocampal volumes as a function of ibuprofen treatment. There was a significant protective effect. There was also a trend towards decreased ventricle size in the ibuprofen-treated and WT animals that was not significant (D). (E) There was a significant correlation between the MRS values of NAA/Cr and the hippocampal volumes in the mice.

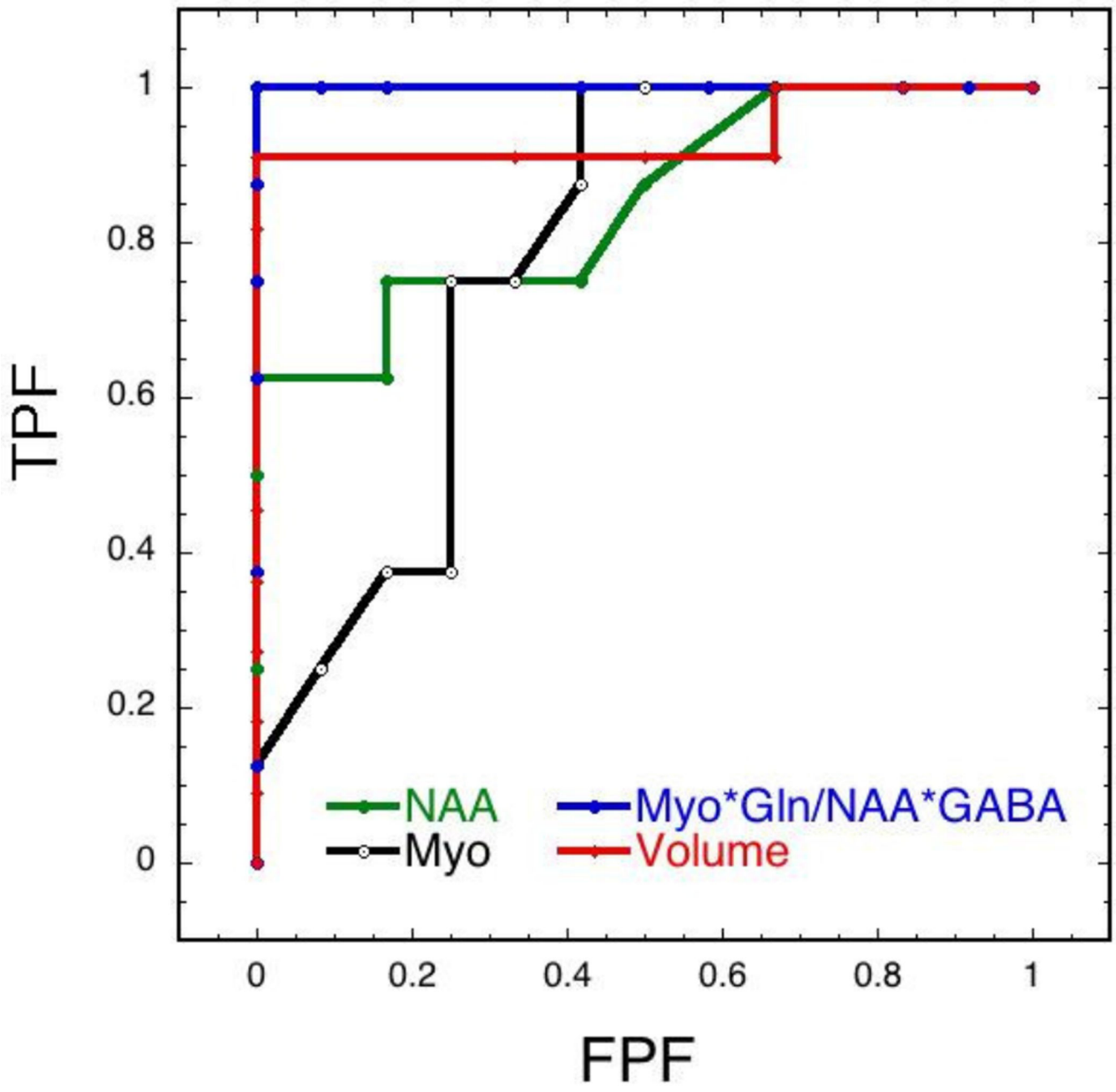

Figure 8.

ROC curves comparing different metrics for classification of the mice. Included were NAA, myo-inositol, myo-inositol*gln/(NAA*GABA) and hippocampal volume. The combined MRS marker yielded the highest area under the curve.

Table 1

Differences Between Triple Transgene Animals Housed in Different Facilities

Chemical/Cr	WT (I) (n=10)	AD (I) (n=9)	WT (II) (n=12)	AD (II) (n=8)
Asp	0.294±.06	0.397±.08¶¶	0.354±.07	0.315±.065*
GABA	0.301±.063	0.312±.056	0.48±.074***	0.355±.065¶¶
Glu	0.69±.061	0.683±.097	0.725±.129	0.752±.036
Gln	0.391±.07	0.412±.036	0.462±.037**	0.473±.048**
Myo-inositol	0.504±.100	0.646±.064¶¶	0.51±.082	0.601±.050¶
NAA	0.459±.067	0.468±.018	0.612±.032***	0.561±.065***¶¶
Taurine	1.041±.148	0.95±.228	0.66±.158***	0.76±.087*

*Differences between WT (I) and WT (II) and AD (I) and AD (II);

*p<0.05;

**p <0.01;

***p<0.001.

¶Differences between AD and appropriate WT;

¶p<0.05;

¶¶p <0.01.

Other chemicals such as lactate, acetate, alanine etc. showed no significant differences between any of the groups. Group I animals had an average age of 17.3 months vs. the group II animals of 18 months.

Table 2

Areas under the curve for ROC classifiers separating AD from WT animals.

Classifier	**AUC Hippocampus**	**AUC Frontal Cx APP×PS1 (Choi et al., 2010a)**
GABA	0.94	ND
NAA	0.84	0.86
Myo (old)	0.78	0.88
Myo (young)	0.91	ND
Myo/NAA	0.95	0.90
Myo*Gln/NAA*GABA	1.0	0.92*
Hippocampal Volume	0.93	ND

* Since GABA does not decline in the APP×PS1 mice but glutamate does we used myo*gln/NAA*glu in the PS×APP mice.